LOW FREQUENCY ARRAY PERFORMANCE
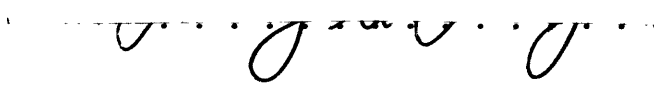IN
SHALLOW WATER

by

DAVID GARDELS OLSON

B.S., Purdue University
(1961)

SUBMITTED IN PARTIAL FULFILLMENT
OF THE REQUIREMENTS FOR THE
DEGREE OF MASTER OF
SCIENCE
at the
MASSACHUSETTS INSTITUTE
OF
TECHNOLOGY
June, 1963

Signature of Author
    Department of Meteorology, May 17, 1963

Certified by

Accepted by . . . .
    Chairman, Departmental Committee on
    Graduate Students

LOW FREQUENCY ARRAY PERFORMANCE
IN
SHALLOW WATER

by

DAVID GARDELS OLSON

Submitted to the Department of Meteorology on May 17, 1963 in partial fulfillment of the requirement for the degree of Master of Science in Oceanography.

ABSTRACT

This thesis investigates the performance of a linear, simply-compensated array in a low-frequency, shallow water sound environment. The problem received attention in this paper because present trends in antenna design and the use of low-frequency sound may cause operational errors in shallow water. The paper follows an analysis by Officer to show the existence of a dispersive system for low-frequency sound in shallow water. The characteristics of a dispersive medium and a simply-compensated array were combined to derive expressions showing the magnitude of bearing determination errors and the loss of array gain for pure tones. Graphs have been prepared to assist a designer in estimating possible errors in such an antenna system.

Thesis Supervisor:

Dr. Donald Ross
Visiting Lecturer,
Department of Naval Architecture
and Marine Engineering

Prof. Henry Houghton
Head, Department of Meteorology

TABLE OF CONTENTS

TABLE OF CONTENTS

LIST OF FIGURES

LIST OF FIGURES

Chapter 1

INTRODUCTION

Description of the Problem

Dispersive characteristics of low-frequency, shallow water transmission can destroy a simply-compensated, or electrically-steered, antenna's ability to detect a sound signal and to infer its direction.

The problem commands interest because of past sound systems and present trends in passive underwater sound arrays. The problem only occurs with antennas that change the direction of their response patterns by electrically adjusting the phase delay between the elements before adding all element outputs. If an antenna is mounted underwater and mechanically turned to "look" in all directions of interest, the problem in this thesis does not exist. The short explanation of these conditions rests with improper knowledge of the sound phase velocity. The exact nature of the problem follows in chapter three and four.

When passive antenna systems grew large, as did some radar systems, the mechanical problem of rotating them was solved by rotating the response pattern instead of the physical configurations. The German Navy employed a high-frequency array mounted along the length of a ship. For obvious reasons electrical steering of the response pattern was mandatory. No problem was encountered because no dispersive system existed. The antenna was used in a high-frequency, deep water environment.

After World War II more emphasis was placed on low-frequency
sound propagation. Transmission attenuation (neglecting reflections
and scatter) is proportional to (frequency)$^{3/2}$ at lower and middle
sound frequencies. Thus, an obvious way to increase operational
range is to lower the operating frequency. The passive system will
detect a low-frequency signal at a longer range than a high-
frequency signal with all other things equal.

If a low-frequency antenna system is placed in shallow water
and electrically steered, the problem outlined in this thesis will
limit the effectiveness of the antenna. The corresponding problem
would occur in electromagnetic systems if a radar antenna were
operated in a wave guide.

Defining the Low-Frequency, Shallow Water Case

Before commenting on the assumptions, the low-frequency,
shallow water case will be defined. At the end of chapter two
the non-dimensional ratio λ_{η}/H (sound wavelength to water depth) is
used to show dispersion effects. Values greater than 0.2 can surely
be considered as shallow water. (See Figures II-V.) Even the ocean
off the continental shelf can appear quite shallow to a sound wave
of one cycle per second (this corresponds to a wavelength of about
5,000 feet). The following diagram will specify the border between
the high- and low-frequency case in this thesis for a sound propaga-
tion velocity of 5,000 feet per second.
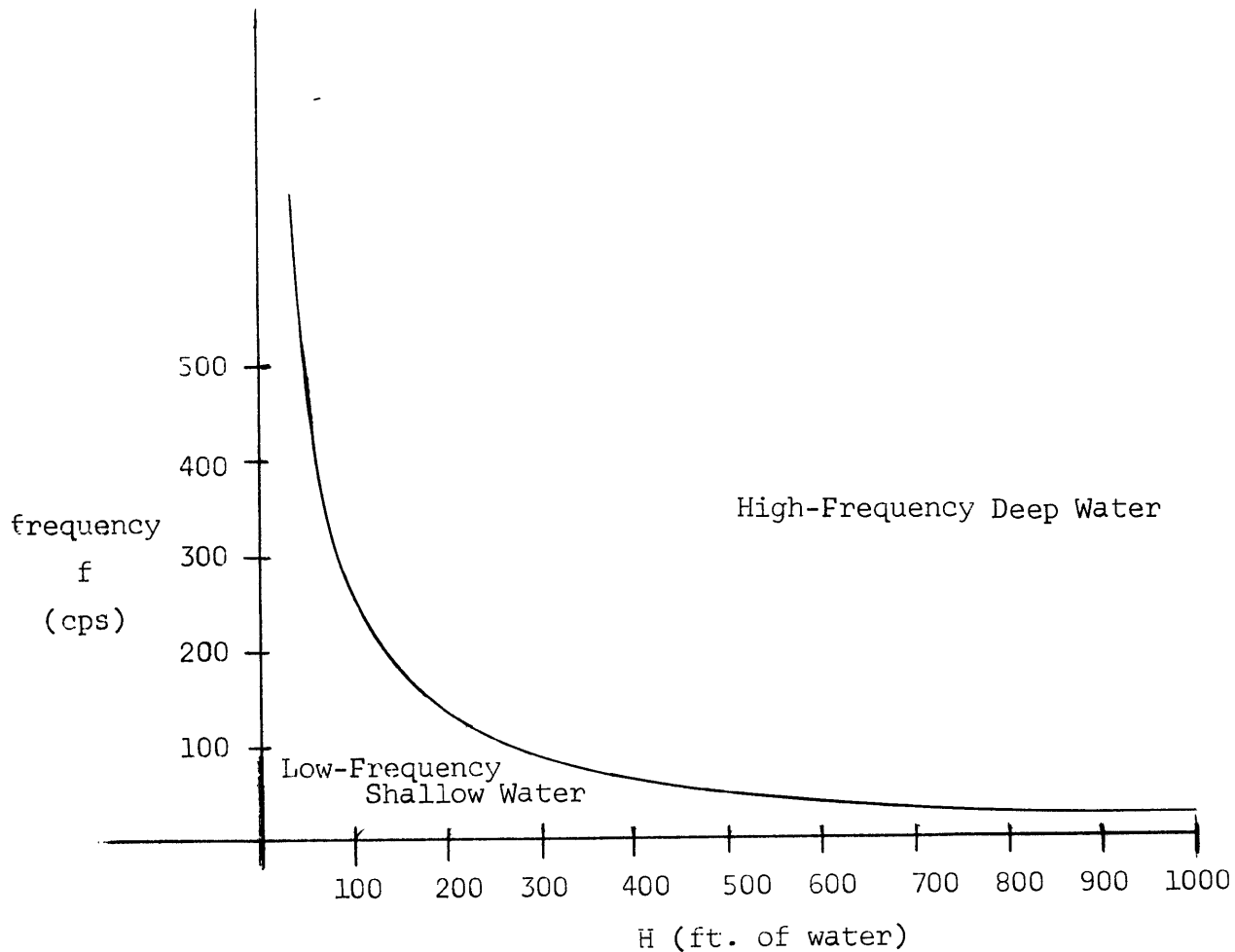
Defining the Different Sound Velocities

The velocity of sound propagation in constant sound velocity

water would be c_1 if $\lambda/H \longrightarrow 0$. This condition is satisfied

at high enough frequencies or deep enough depths in accordance to

the preceding diagram. The "deep ocean" sound velocity is then

defined as c_1. The sound velocity in the ocean floor is defined as

c_2. Chapter two will show that the sound phase velocity, or

velocity of wave propagation, is a function of frequency in a

dispersive medium. This velocity as a function of angular frequency

is defined $V(\omega)$. In this thesis a deep water antenna refers to an antenna designed in accordance to a constant sound phase velocity c_1. Data[1] demonstrates that a fine sand bottom has typical ratios of c_2/c_1 and ρ_2/ρ_1 of 1.11-1.16 and 2 respectively. Some mixtures of bottom material and water result in lower bottom velocities than the deep ocean sound velocity. Marsh and Schulkin[2] point out that bottom properties are controlling and further state that the principal problem in calculating the shallow water sound field is the lack of detailed knowledge of c_2.

Assumptions

Variations in the model parameters will alter local conditions and change transmission between two points (i.e., intensity, arrival time, and the exact pattern of the standing vertical wave); however, these variations do not change the essential and critical feature of low-frequency, shallow water sound transmission (i.e., the bottom and surface reflections of sound waves cause dispersion). Therefore, the usual variations of temperature and salinity, sea-state, and bottom smoothness were neglected because they are unimportant in this particular problem. Only a few assumptions were necessary to facilitate analysis and computation. These are stated below:

1. The water itself has a constant sound propagation velocity.

---

1. See pages 4-5 in Reference (5).
2. See page 65 in Reference (7).

2. The ocean bottom density and the velocity of
   sound propagation in the ocean bottom were taken
   as greater than the sound velocity and density
   of the ocean water.

3. The model assumed a "far field" condition where
   the distance between the sound source and the
   antenna was large compared to the antenna
   dimensions. Attenuated sound modes do not reach
   the antenna.

4. The impinging sound waves were assumed plane.

5. The model assumed that bottom and surface reflec-
   tions from sound ray angles greater than the
   critical angle were not attenuated. (The critical
   angle is $\phi crit = \arc \sin (c_1/c_2)$.)

Justification of the Assumptions

The first assumption has no relevance concerning the existence
of dispersion; but, the use of a constant c_1 in future calculations
eases computation. If water is free from large salinity variations
and wind mixes the water, an isothermal, isovelocity sound field
can be a very good assumption when the water depth does not exceed
200 feet. The data mentioned previously in Reference (5) justifies
assumption (2). The fourth assumption follows from assumption (3)
since the radius of curving waves approaches infinity in the far
field. The fifth assumption is a property of the dispersive system
covered by Officer and further mentioned in Chapter two.

Past Work Concerning Dispersive Systems

Several authors such as Officer and Tolstoy[3] have considered
the shallow water dispersive system. Tolstoy states that if a
medium is bounded by reflecting walls, it will act as a wave guide.
Energy from a sound source gets permanently trapped by a process of
continuing total reflection (unattenuated modes). The guided energy
spreads cylindrically and constitutes the dominant arrival at long
ranges within the guide.

Tolstoy further states that the propagation of guided waves
is dispersive and one must distinguish between phase velocity $V(\omega)$
and group velocity $U(\omega)$. If k is the wave guide number parallel to
the reflecting surfaces, these two velocities are defined:

$$V(\omega) = \frac{\omega}{k}$$

$$U(\omega) = \frac{d\omega}{dk} \quad \text{(for the transient case)} .$$

$U(\omega)$ gives the energy propagation velocity along the guide of
energy contained in a band width $d\omega$ centered about a mean frequency
ω. The phase velocity $V(\omega)$ is the "instantaneous" velocity of a
point of constant phase as measured by two detectors.

Clay[4] used the work of Tolstoy to investigate array steering
in a layered wave guide. He uses a two element array that takes

---

3. See Reference (11).

4. See Reference (4).

the time average of the square of the sums of the element outputs
and infers the sound source direction when the phase delay is
adjusted to yield a maximum. The cross-term is the covariance of
the two pressure signals. This cross-term contains the directional
information; but it has several maxima and minima (instead of one
maxima for the deep water system) since the group velocity changes
with frequency and mode. The complications of multiple maxima are
caused by constructive and destructive interference of the covariance
functions of several modes. The multiple maxima cause ambiguous
bearing determinations for the sound source.

Clay obtains a numerical solution for a simple source by
further use of Tolstoy's work. This thesis begins its treatment
by considering a system that infers direction by sensing the phase
arrivals of the sound wave. The antenna elements sense pressure
variations (compression and rarefaction), and electrically-steered
antennas are adjusted to sample the same portions of the wave. The
wave front moves with a phase velocity $V(\omega)$ which is not a constant
in a dispersive system. A bundle of sound energy consisting of many
frequencies moves with group velocity $U(\omega)$; but the frequency
components move with phase velocity $V(\omega)$, so the bundle changes
shape since $V(\omega) > U(\omega)$. If the bundle moves far enough, the low
frequencies arrive first, followed by higher frequencies.

This thesis begins analysis with a pure-tone sinusoidally
varying sound signal. The thesis will demonstrate the existence

and quantitative measurement of the bearing error and loss of array gain experienced by a deep water, simply-compensated antenna in a low-frequency, shallow water sound field.

Chapter 2

THE SHALLOW WATER ENVIRONMENT

Types of Dispersion

In shallow water the reflections of sound waves from the ocean bottom and the air-water interface create a geometrical dispersive medium. If dispersion is caused by a spatial velocity variation in a continuous or discontinuous manner across boundaries, it is called geometrical dispersion. If dispersion is caused by a dependence on frequency of the physical parameters determining the wave velocity, it is called material dispersion.

The method outlined by Officer[5] will calculate the dependence of the sound phase velocity as a function of frequency for geometrical dispersion. The case for material dispersion was stated in Reference (7). The relaxational absorption in sea water changes sound speed with frequency. One computation shows a maximum dispersion effect of 2-4 cm/sec.[6] This small effect will not be considered in comparison to the larger effects of material dispersion for low-frequency, shallow water sound.

Normal-Mode Solution

In the deep ocean a normal-mode solution often becomes awkward (although Carter demonstrates that it may be more useful than previously thought in Reference (2)). For the shallow water case the

---

5. See Reference (8).

6. See page 30 in Reference (7).

normal-mode solution can be computed with more ease. In fact the normal-mode solution is the only acceptable method, since the ray solution is invalid when a standing wave pattern exists. The conditions necessary for the Eikonal equation to satisfy the wave equation are violated, and the ray solution cannot be used to predict the existence of a dispersive wave train.

In a dispersive medium the velocity of wave propagation, or the phase velocity, depends on the frequency and modes of vibration in which the sound signal is propagating. This dependency is shown for a specific set of parameters in Figure I. The phase velocity $V(\omega) = c_1/\sin \phi$. The critical angle ϕ crit = arc sin c_1/c_2 is defined as the angle where complete reflection begins for ϕ crit $\leq \phi \leq \pi/2$. Plane waves more incident than ϕ crit are attenuated. The expression $V(\omega)$ applies only to angles of ϕ greater than ϕ crit.

In general a sound wave striking a density and propagation velocity discontinuity will divide into a reflected and a refracted wave. Examples of these discontinuities are the sea-ocean bottom interface and the air-sea interface at the ocean surface. When a plane wave in the ocean strikes the air-sea interface, the sound wave is completely reflected with a phase change of π or 180°.[7]

_____

7. See page 31 in Reference (9).

Figure I

DISPERSION CURVE: Phase Velocity vs. Frequency

for $C_2/c_1 = 1.15$ (n - mode number)
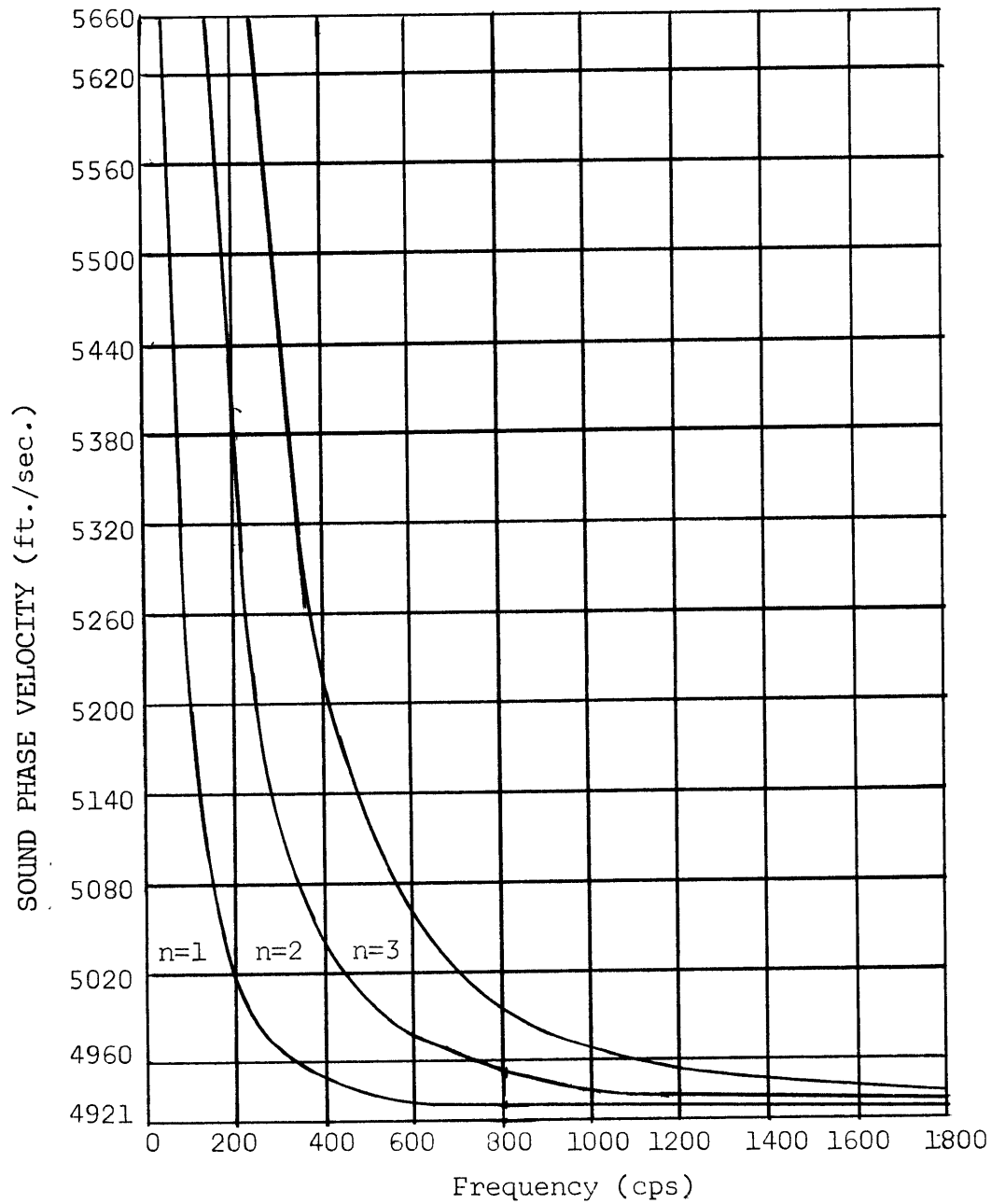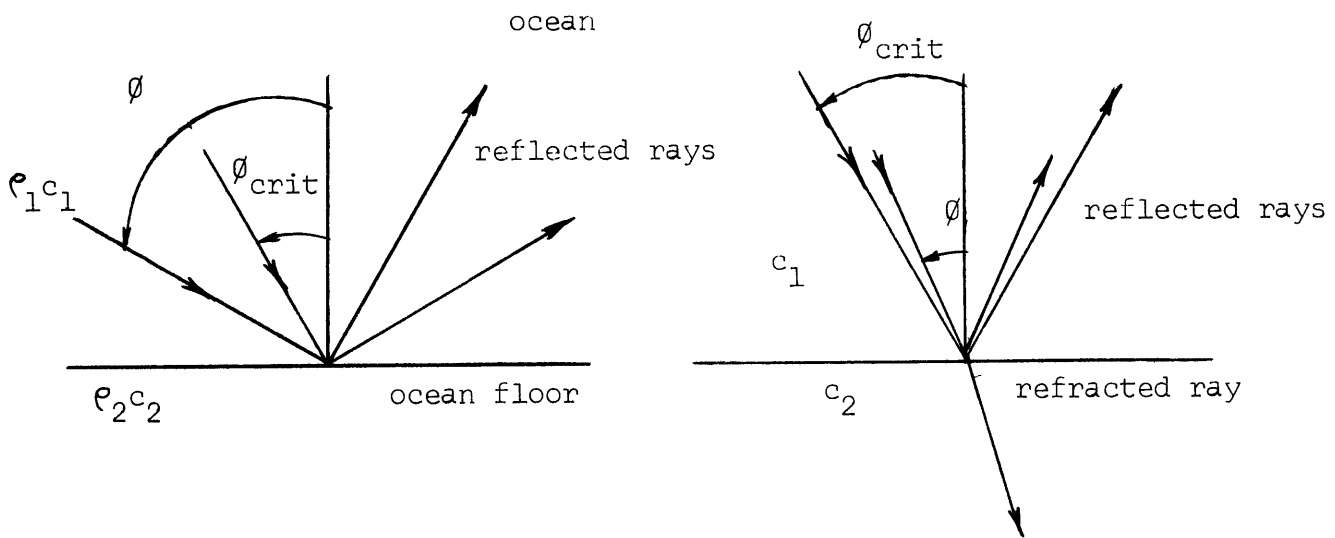
At all angles of incidence equal to or greater than ϕ crit

there is no attenuation of the reflected plane sound wave since no

sound energy is refracted into the bottom. Reflected sound waves

with $\phi < \phi$ crit are attenuated and thus neglected in this far field

model. The impinging sound wave will undergo a phase change upon

reflection according to[8]

$$\frac{\Sigma}{2} = \text{arc tan} \ \frac{\rho_1}{\rho_2} \frac{\sqrt{\sin^2\phi - (c_1/c_2)^2}}{\cos \ \phi}$$

8. See page 79 in reference (8).

The phase change Σ depends on the angle of incidence $\emptyset$ and varies

between 0 and π radians for $\emptyset$ crit and $\emptyset = \pi/2$ radians respectively.

The multiply-reflected rays will form standing waves in the

vertical direction because of the phase additions of the sound waves.

The vertical patterns of these standing waves show the modes of

sound propagation. The relation between the angle of incidence $\emptyset$

of a group of multiply-reflected rays and the set of prominent

discrete frequencies associated with this angle is given by[9]

$$\frac{2\pi f_n H \cos \emptyset}{c_1} - \frac{\Sigma}{2} = (2n-1) \frac{\pi}{2} \ ,$$

and n is the mode number where

$$n = 1, 2, 3, ---\ .$$

Interpreting the $\frac{\lambda n}{H}$ Plots

Four graphs were prepared to show the effects of dispersion.

Each graph has a different c_2/c_1 ratio, but the ρ_1/ρ_2 ratio was

held constant at 0.5. The expressions showing the dependence of

phase velocity on frequency were altered to obtain a non-dimensional

ratio λ_n/H (n refers to the mode) to plot versus $K(\omega) = \frac{V(\omega)}{c_1} -1.$

Now $$\lambda_n = \frac{V(\omega)}{f_n} \ .$$

---

9. See pages 117-122 in Reference (8).

Using the expression giving f_n, we can get

$$f_n = \frac{\left[(2n-1)\frac{\pi}{2} - \frac{\Sigma}{2}\right] c_1}{2\pi H \cos \emptyset}$$

Thus in terms of the angle of plane wave incidence on the ocean floor and surface $\emptyset$, the quantities

$$\frac{\lambda n}{H} = \frac{2\pi \cot \emptyset}{\left[(2n-1)\frac{\pi}{2} + \frac{\Sigma}{2}\right]} \quad \text{and} \quad \frac{V(\omega)}{c_1} - 1 = \left(\frac{1}{\sin \emptyset} - 1\right).$$

can be calculated for plotting.

The ratio of c_1/c_2 specifies the critical angle for unattenuated wave propagation as $\emptyset$ crit = arc sin (c_1/c_2). This condition then in part with the water depth specifies the cut-off frequency since f_n is not calculated for $\emptyset < \emptyset$ crit. In the graphs the plot ends when $K(\omega) = (c_2/c_1 - 1)$ since the greatest value of $V(\omega)$ for any given case is c_2. The ratio of $\frac{\lambda n}{H}$ for each mode at $K(\omega) = c_2/c_1 - 1$ specifies the cut-off frequency for each mode of unattenuated propagation. The wave duct acts as a high-pass filter.

Approximating the $\frac{\lambda n}{H}$ Versus $K(\omega)$ Curve

The calculations for Figures II-V were very time consuming and laborious. For engineering work where graphs of this type could show the magnitude of dispersive effects and the number of allowable modes, an approximation would be valuable. If the ratio of c_1/c_2 and the water depth H can be measured, the cut-off points can be

calculated and the range of $V(\omega)$ known. Since a relation between

$\emptyset$ and $\dfrac{V(\omega)}{c_1}$ exists, the $\emptyset$ terms may be eliminated. The phase

change Σ ranges from 0 to $180°$. If $V(\omega)$ is specified as $\dfrac{c_1+c_2}{2}$,

an intermediate range approximation for $\dfrac{\lambda n}{H}$ can be made.

From before

$$\tan \frac{\Sigma}{2} = \frac{\rho_1}{\rho_2} \frac{\sqrt{\sin^2 \emptyset - (c_1/c_2)^2}}{\cos \emptyset}$$

$$= \frac{\rho_1}{\rho_2} \frac{\sqrt{1 - \left(\frac{V(\omega)}{c_2}\right)^2}}{\sqrt{\frac{V(\omega)}{c_1}^2 - 1}} \quad .$$

Using $V(\omega) = \dfrac{c_1+c_2}{2}$,

$$\tan \frac{\Sigma}{2} = \frac{\sqrt{3 - (\frac{c_1}{c_2})^2 - 2(\frac{c_1}{c_2})}}{\sqrt{\left(\frac{c_2}{c_1}\right)^2 + 2\frac{c_2}{c_1} - 3}}$$

Use this value for obtaining

$$\frac{\Sigma}{2} \quad .$$

Now taking

$$\frac{\lambda_n}{H} = \frac{2\pi \cot \phi}{(2n-1)\frac{\pi}{2}\left[1 + \dfrac{\Sigma/2}{(2n-1)\frac{\pi}{2}}\right]}$$

rearrange to get

$$\left(\frac{\lambda_n}{H}\right)^2 \frac{\left[(2n-1)\right]^2}{32\left(1+\frac{K(\omega)}{2}\right)}\left[1 + \frac{\Sigma/2}{(2n-1)\frac{\pi}{2}}\right]^2 = K(\omega) \qquad .$$

The final form using the chosen value of $V(\omega)$ for $1 + \dfrac{K(\omega)}{2}$ becomes

$$K(\omega) = \left(\frac{\lambda_n}{H}\right)^2 \frac{\left[(2n-1)\right]^2}{32\left[\frac{3c_1 + c_2}{4c_1}\right]}\left[1 + \frac{\Sigma/2}{(2n-1)\frac{\pi}{2}}\right]^2 .$$

A curve using $c_2/c_1 = 1.15$ and $\rho_1/\rho_2 = 0.5$ and this approximation was drawn in Figure VI. As the mode number n increases, the approximation becomes better because the term containing $\frac{\Sigma}{2}$ becomes smaller. Comparing Figure IV with Figure VI will demonstrate the accuracy of this approximation.

Figure II

NON-DIMENSIONAL DISPERSION EFFECTS CURVE:
Wave Length to Water Depth Ratio ($\frac{\lambda n}{H}$) vs.
Fractional Change of Phase Velocity to Deep
Ocean Velocity ($K(\omega)$) for $c_2/c_1 = 1.05$, $\rho_2/\rho_1 = 2$

(n - mode number)
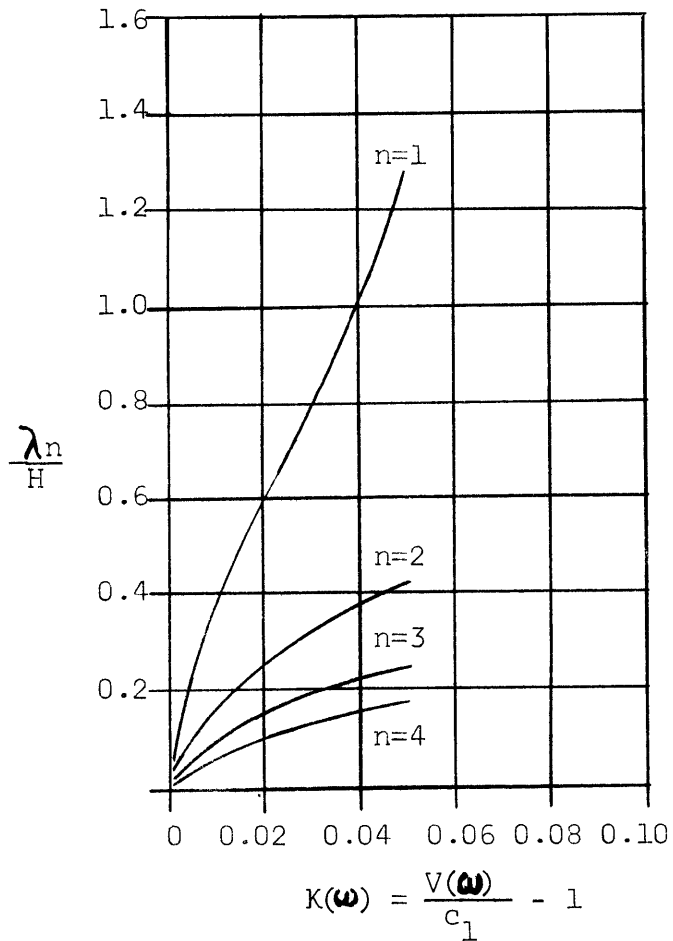
$$K(\omega) = \frac{V(\omega)}{c_1} - 1$$

Figure III

NON-DIMENSIONAL DISPERSION EFFECTS CURVE FOR

$$c_2/c_1 = 1.10 , \rho_2/\rho_1 = 2$$

(n - mode number)
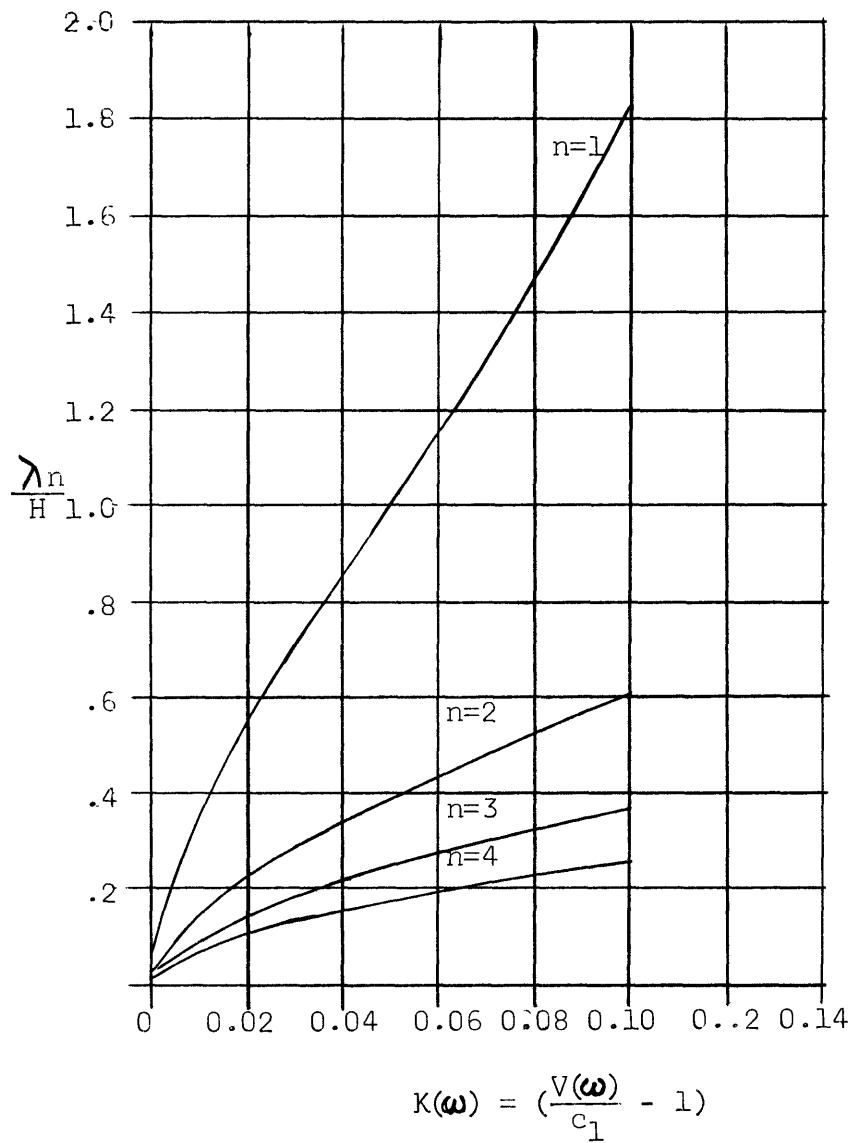
$$K(\omega) = (\frac{V(\omega)}{c_1} - 1)$$

Figure IV

NON-DIMENSIONAL DISPERSION EFFECTS CURVE FOR

$$c_2/c_1 = 1.15 \ , \ \rho_2/\rho_1 = 2$$

(n - mode number)

$$K(\omega) = (\frac{V(\omega)}{c_1} - 1)$$

Figure V

NON-DIMENSIONAL DISPERSION EFFECTS CURVE FOR

$c_2/c_1 - 1.20$, $\rho_2/\rho_1 = 2$
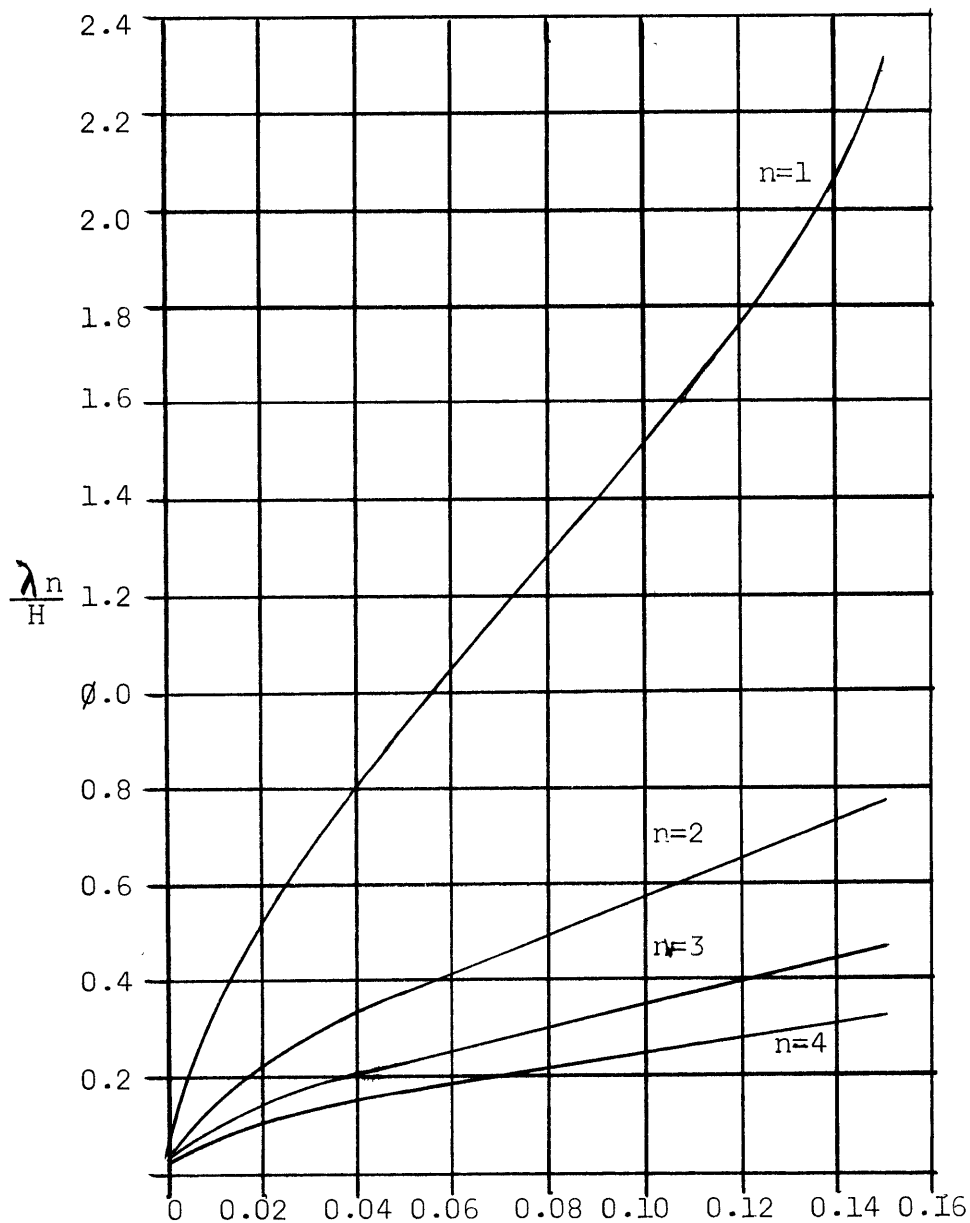
(n - mode number)

$K(\omega) = (V(\omega)/c_1 - 1)$
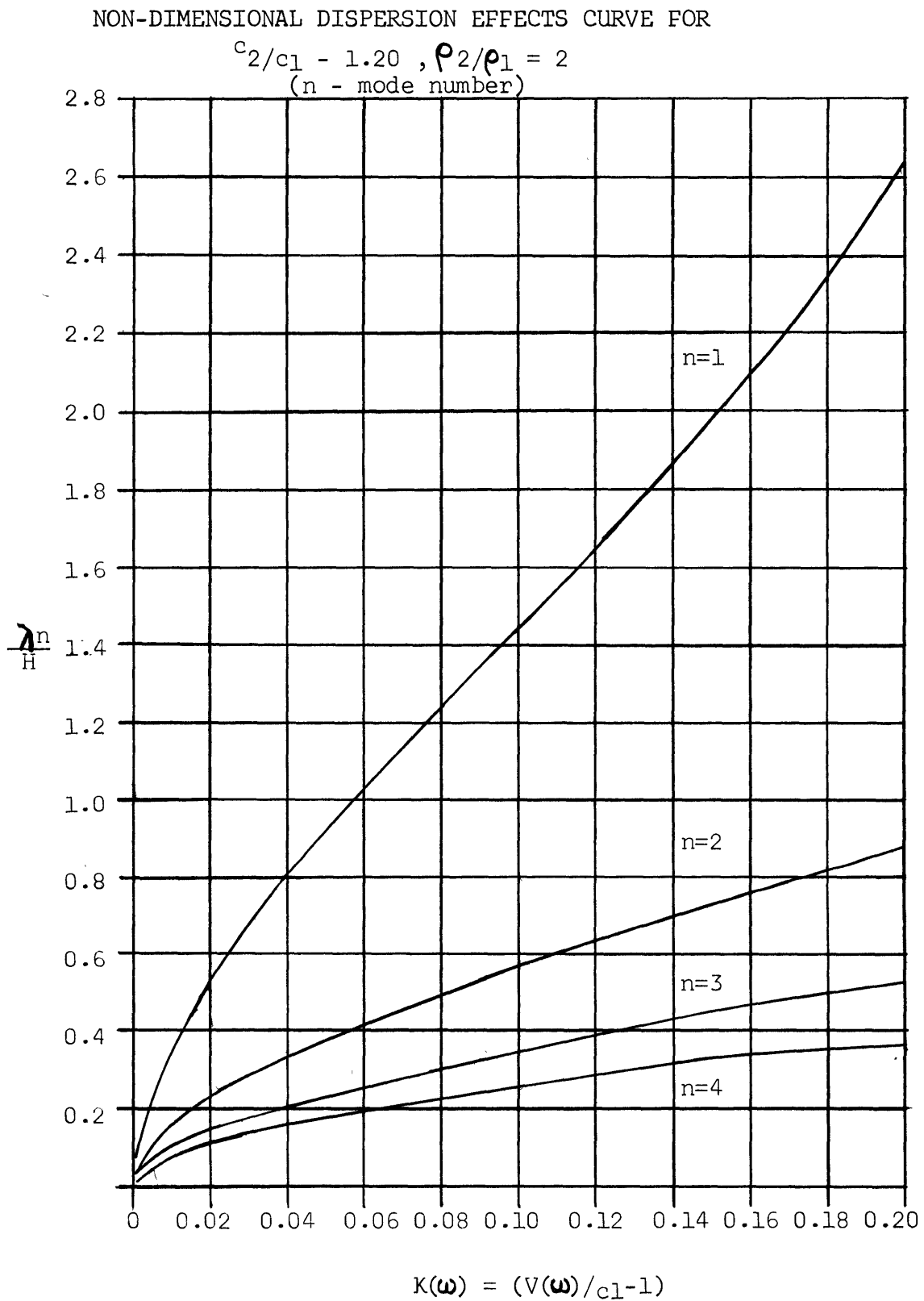
Figure VI

APPROXIMATED NON-DIMENSIONAL DISPERSION EFFECTS CURVE FOR
$$c_2/c_1 = 1.15, \quad \rho_2/\rho_1 = 2$$
(n - mode number)

$$K(\omega) = (\frac{V(\omega)}{c_1} - 1$$
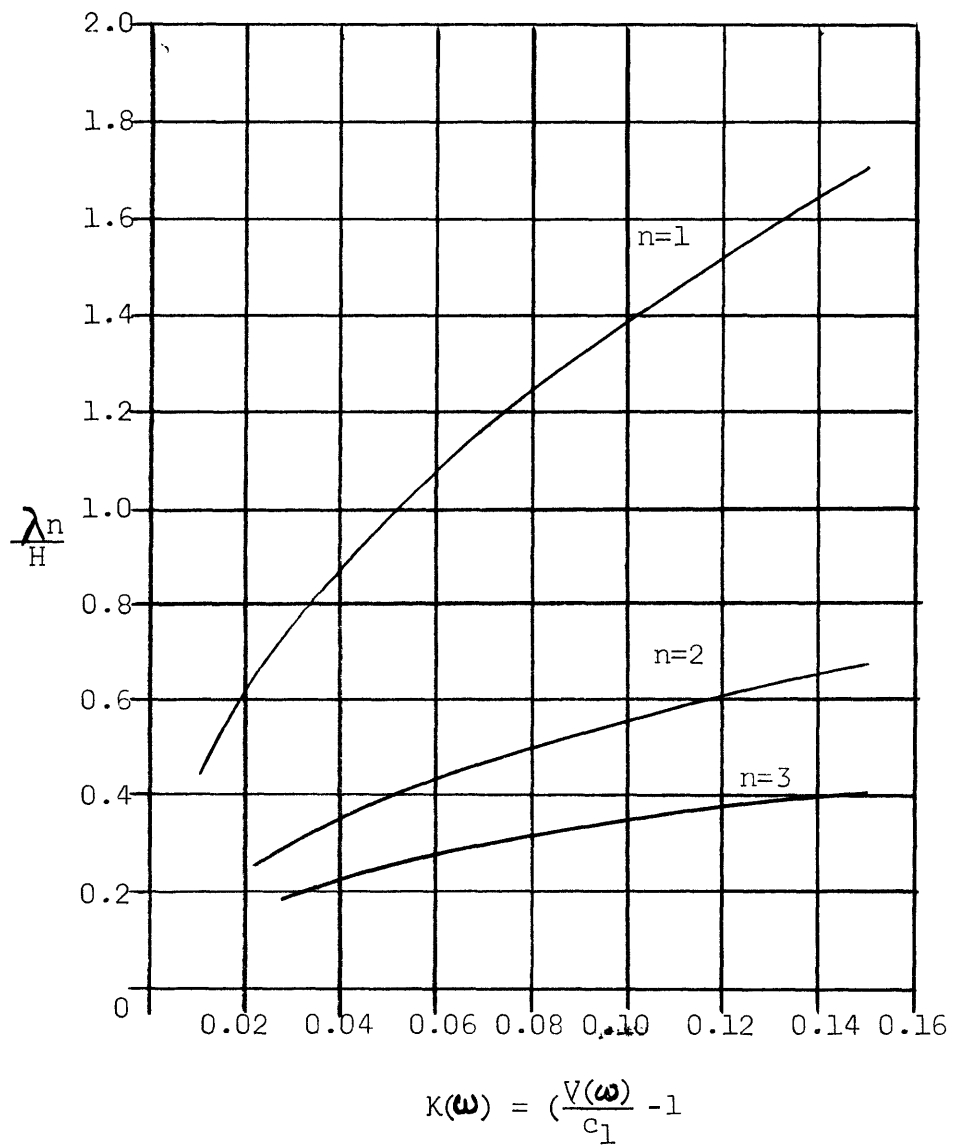
Chapter 3
THE ANTENNA SYSTEM

Antenna Description

A directive receiving array, or antenna, is designed to detect the presence of a sound signal and to infer the direction of the signal from the array in an underwater sound field. The antenna system of interest consists of hydrophones (transducers capable of transforming sound in water into electrical signals) arranged in a line along the ocean floor.

Before proceeding with the discussion some variables must be defined:

θ - the angle between the ray in the direction
of sound propagation (this ray is perpendicular
to the plane waves) and the perpendicular to
the array line
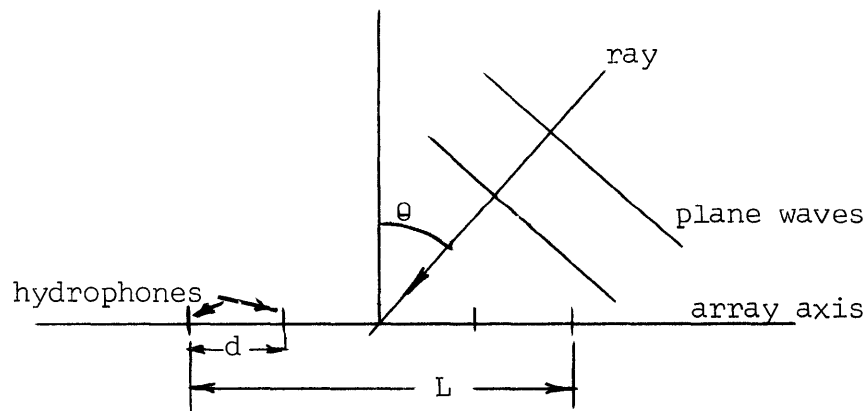
(When $\theta = 0$ the signal is approaching from "broadside" and at $\theta = \frac{\pi}{2}$ the signal is located at "endfire" to the array.)

$\omega = 2\pi f$ - the angular frequency of the sound signal

$\quad\quad$ x - the position along the antenna (The center

$\quad\quad\quad$ of the antenna is taken as x = 0.)

$\quad\quad$ d - the spacing distance between hydrophones

$\quad\quad\quad$ in the antenna

$\quad\quad$ L - the total length of the antenna

$\quad k = \dfrac{\omega}{c_1}$ - the wave number in a deep ocean

$\gamma = \dfrac{\omega}{c_1} \sin\theta$ - the trace wavelength in a deep ocean

Antenna-Signal Processing Analogy

A close analogy between the antenna system and electric signal

processing terminology can be exploited to explain the functions

and characteristics of the underwater antenna. The antenna detect-

ing a sinusoidal sound signal in a noise field will be explained

as the analog of a periodically-spaced, unit-impulse train cross-

correlated with an electric noise signal to detect the presence of

a sinusoidal electrical signal. The antenna performs spatial

filtering as the counterpart to time filtering in the electrical

signal processing analog. The principal analogous terms must now

be defined:

Antenna System	Electrical Signal Processing
trace wavelength	angular frequency ω
position on the array x	time t
sensitivity at a point	voltage at a time
radiation pattern	power spectral density
sensitivity function $h(x,\omega)$	unit-impulse response $h(t)$
sensitivity spectrum $H(\gamma,\omega)$	system function $H(\omega)$

The sensitivity function h(x,ω) gives the antenna response to a pure-tone pressure signal of angular frequency ω at the point x on the antenna. A common set of units are volts per unit pressure per unit length of the array.[10] It now becomes important to see how the sensitivity of the array to sound signals varies in space. Consider an n-element antenna of equally-sensitive hydrophones equally-spaced a distance d apart. The total length of the array is L = (n-1) d.

The sensitivity spectrum is the Fourier transform of the sensitivity function:

$$H\ (\gamma,\omega) = \int_{-\infty}^{\infty} h(x,\omega) \exp\ (-j\gamma x)\ d\ x$$

$$h(x,\omega) = \frac{1}{2\pi} \int_{-\infty}^{\infty} H\ (\gamma,\omega) \exp(j\gamma x)\ d\gamma \qquad .$$

The response function $\left| H(\gamma,\omega) \right|^2$ plotted against γ and normalized gives the directive pattern of the antenna. The equally-spaced, equally-sensitive hydrophones correspond to the unit-impulse train periodically-spaced in time. The equivalent linear system that performs spatial sampling for the detection of a sound signal in a noise background must have a unit response

$$h(x,\omega) = u(x) + u(x-d) + u(x-2d)+----+u\left[x-(n-1)d\right] \qquad .$$

---

10. See Reference (1) for an outline of this treatment.

The sensitivity spectrum can be evaluated as

$$H(\Gamma,\omega) = \int_{-\infty}^{\infty} h(x,\omega) \exp(-j\Gamma x)\, dx$$

$$\int_{-\infty}^{\infty} u(t-kd) \exp(-j\Gamma x)\, dx = \exp(-j\,k\,d\,\Gamma)$$

$$k = (1,\ 2,\text{---}(n-1)).$$

Thus

$$H(\Gamma,\omega) = 1 + \exp(-jd\Gamma) + \exp(-j2d\Gamma) + \text{---} \exp\left[-j(n-1)d\Gamma\right]$$

$$= \frac{1 - \exp(-jnd\Gamma)}{1 - \exp(-jd\Gamma)} \qquad \text{[11]}$$

$$H(\Gamma,\omega) = \left| \frac{\exp\left(\frac{jnd\Gamma}{2}\right) - \exp\left(\frac{-jnd\Gamma}{2}\right)}{\exp\left(\frac{jd\Gamma}{2}\right) - \exp\left(\frac{-jd\Gamma}{2}\right)} \right| = \left| \frac{\sin\left(\frac{nd\Gamma}{2}\right)}{\sin\left(\frac{d\Gamma}{2}\right)} \right|.$$

The normalized directional response pattern is written

$$K(\theta) = \frac{\sin\left(\frac{nkd}{2} \sin\theta\right)}{n \sin\left(\frac{kd}{2} \sin\theta\right)}$$

In this analysis the frequency of the sound wave signal was held

constant for a particular $K(\theta)$.

---

11. See pages 315-318 in Reference (6).

Antenna Response

The positions along the antenna for maximum response to a sound signal occur when $K(\theta) = 1$, the condition for a major lobe. Since n has an integral value, the major lobes occur when $\frac{kd \sin \theta}{2} = 0$. Complete nulls for signal response occur along the antenna when $\frac{n \; kd \sin \theta}{2} = m\pi$ $\quad$ m = (1, 2, 3,---n). Between $\frac{kd \sin \theta}{2} = 0$ and $\frac{kd \sin \theta}{2} = \pi$ (the condition for the next major lobe), there are (n-1) nulls. The minor lobes between each null decrease as n (the number of hydrophones) increases according to the expression for $K(\theta)$. The signal response between major lobes can be made small with the result that the signal is only received at a point on the antenna corresponding to a major lobe.

Since the major lobes are equal, reception of signals will be ambiguous with respect to location along the array if more than one major lobe exists. The major lobes are located at (n-1) $\frac{kd \sin \theta}{2} = \pi n$ or using a maximum value of γ at $\theta = \frac{\pi}{2}$, the first ambiguous major lobe occurs at $\frac{2\pi n}{L} = \gamma$. So for $k < \gamma$ and no ambiguous lobes, we require $\frac{2\pi n}{L} > k = \frac{2\pi}{\lambda}$ or a maximum spacing at broadside of $\frac{L}{n} < \lambda$. Since we desire to steer the array so that the major lobe is not always pointing to broadside, the condition allowing the major lobe to be steered to endfire without ambiguous modes requires

$$\frac{L}{n} < \frac{\lambda}{2} \qquad \cdot^{12}$$

---

12. See pages 23-24 in Reference (1).

In the preceding paragraph the concept of steering the major

lobe was mentioned. This is done by timing the hydrophones to

add their outputs as a plane wave successively sweeps past them.

For a plane wave coming from an angle θ the time delay between

hydrophone addition must be $\dfrac{d \sin \theta}{c_1} = \tau$ in a completely homogeneous,

deep ocean.
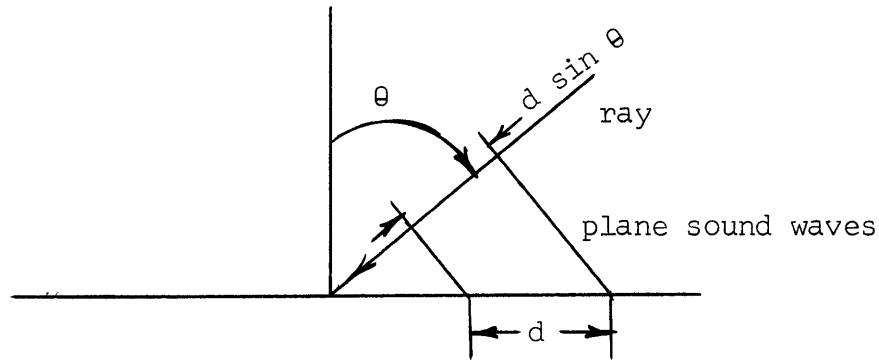
Array Gain and Directivity

The array gain is defined as the signal to noise ratio of

the antenna divided by the signal to noise ratio of one hydrophone.

If the background noise is homogeneous (invariant with changes in

position and time), an n element array has an array gain n (not in

decibels).

An isotropic wave field results from uncorrelated plane

sound waves incident on the antenna from all directions with equal

intensity. The directivity D of an array is the array gain when

the signal is a plane wave coming from the direction producing

maximum output in an isotropic wave field. The directivity equals

the reciprocal of the average value of $\left| H(\gamma, \omega) \right|^2$ in the range

of γ corresponding to incident plane waves ($-k < \gamma < k$) when the pattern is normalized.

$$D = \frac{\left| H(\gamma,\omega) \right|^2 \, max}{\int_{-k}^{k} \left| H(\gamma,\omega) \right|^2 \, d\gamma}$$

In a later section the approximations

$$D \doteq \frac{kL}{\pi} \qquad \text{(not endfire)}$$

$$\text{and} \quad D \doteq \frac{2kL}{\pi} \qquad \text{(endfire)}$$

will be used as an antenna parameter.[13]

Beamwidth

It should be mentioned that the major lobe in the directional response pattern has a finite beamwidth. Some authorities define the beamwidth between the -3db or -6db levels of the major lobe. The beamwidth changes with θ, frequency and n. All changes in θ referred to in this paper are in reference to the axis of the major lobe.

13. See page 13 in Reference (1) and Reference (10).

Equivalence of Continuous and Point Arrays

In future discussions a knowledge that the n-element array can be equivalent to a continuously sensitive line array is useful. An equivalent n-element array has the same sensitivities at its n-element locations as a continuous array of the same length. The n-element array has an equivalent length of nd, where d is the hydrophone spacing, in comparison to its physical length of L=(n-1)d. This means that an n-element array of L=(n-1)d is equivalent to a continuous line array of length L=nd. In the limit of the directional response pattern as n⟶∞, this difference will make no change in the final result.

From before L = (n-1)d, but we shall now use the equivalent length and write L = nd. Then

$$K(\theta)_{\text{continuous array}} = \lim_{n \to \infty} K(\theta)_{\text{point array}}$$

$$K(\theta)_{\text{continuous array}} = \lim_{n \to \infty} \sin \frac{\left(\frac{nkd}{2} \sin \theta \right)}{n \sin \left(\frac{kd}{2} \sin \theta \right)}$$

$$= \lim_{n \to \infty} \frac{\sin \left(\frac{nkL}{n2} \sin \theta \right)}{n \left(\sin \left(\frac{kL}{n2} \sin \theta \right) \right)}$$

$$K(\theta)_{\text{continuous array}} = \frac{\sin \left(\frac{kL}{2} \sin \theta \right)}{\frac{kL}{2} \sin \theta}$$

Chapter 4

THE EFFECTS OF DISPERSION ON ANTENNA PERFORMANCE

Plan of Attack

In chapters two and three the variations of the phase velocity
and the principles of antenna operation were presented. Since an
antenna must detect a signal and infer direction, we should now
look for the effects of the phase velocity on array gain and bearing
determination. First the effect of using the wrong phase velocity
for turning the directional response pattern will be investigated.
Finally the conditions for array gain fall-off will be investigated
as a function of phase velocity and antenna directivity.

Array Steering and Phase Velocity

In order to steer an array electrically the phase velocity of
the sound signal must be known. In the previous description of the
antenna system the deep ocean sound propagation velocity was used.
Now the errors caused by improper knowledge of the phase velocity
can be derived.

In a general case the time delay between adding the outputs of
the successive hydrophones to detect a signal propagating toward
the array at an angle θ to broadside is $\tau = \dfrac{d \sin \theta}{c_1}$. This
expression demonstrates how the determination of θ depends on the
value of the phase velocity:

$$\theta = \text{arc sin} \left(\frac{c_1 \tau}{d}\right) \quad .$$

Obviously, if the value taken as c_1 is incorrect, the computed direction of the sound source is incorrect also.

Now an expression for the correct angle θ will be derived in terms of the incorrect angle θ_1, the incorrect phase velocity c_1, and the correct phase velocity $V(\omega)$.

$$\tau = \frac{d \sin \theta_1}{c_1} = \frac{d \sin \theta}{V(\omega)}$$

$$V(\omega) \sin \theta_1 = c_1 \sin \theta$$

Since the correct phase velocity always exceeds or is equal to c_1, the correct angle θ always exceeds or equals the incorrect θ_1. Therefore, express $\theta = \theta_1 + \Delta\theta$ where $\Delta\theta$ is the error in direction determination of the axis through the major lobe of the directional response pattern. Thus

$$\frac{V(\omega)}{c_1} \sin \theta_1 = \sin (\theta + \Delta\theta)$$

Subtract $\sin \theta_1$ from each side and divide each side of the resulting equation by $\Delta\theta$. Using the general definition for the derivative of a function, the result becomes

$$\Delta\theta = K(\omega)\tan \theta_1 \text{ where } K(\omega) = \frac{V(\omega)}{c_1} - 1 \quad .$$

Using sample data where $c_2/c_1 = 1.15$, the maximum error at $\theta_1 = 45°$ is

$$\Delta\theta = .15 \text{ rad.} \quad \text{or}$$

$$8° \ 35' \quad .$$

Figure VII shows the relation between $K(\omega)$ and θ_1 for errors of $3.5°$ and $7°$.

Array Gain Loss

When the sound source is really located at endfire, there is no value of θ_1 to correlate with the incorrect time delay between hydrophones. When the sound source is at endfire and the antenna system "thinks" it is looking at some θ_1 less than $90°$, the array gain falls off because the hydrophones are not adding coherently.

In the dispersive medium the true representation of the sound signal in space and time is

$$p(x,t) = p_o \cos\left(\omega t - \frac{\omega x \sin\theta}{V(\omega)}\right) .$$

In a non-dispersive medium this was previously written

$$p(x,t) = p \cos(\omega t - \gamma x) \text{ where}$$
$$\gamma = k \sin\theta .$$

The phase error is contained in the spatial component of $p(x,t)$. The phase error at any point x_o is

$$\text{Phase Error} = \frac{\omega x_o \sin\theta}{c_1} - \frac{\omega x_o \sin\theta}{V(\omega)}$$

$$= k x_o \left(1 - \frac{c_1}{V(\omega)}\right) \sin\theta \quad .$$

Figure VII

THE BEARING DETERMINATION ERROR CURVE:

As A Function of Steering Angle θ_1 and $K(\omega)$
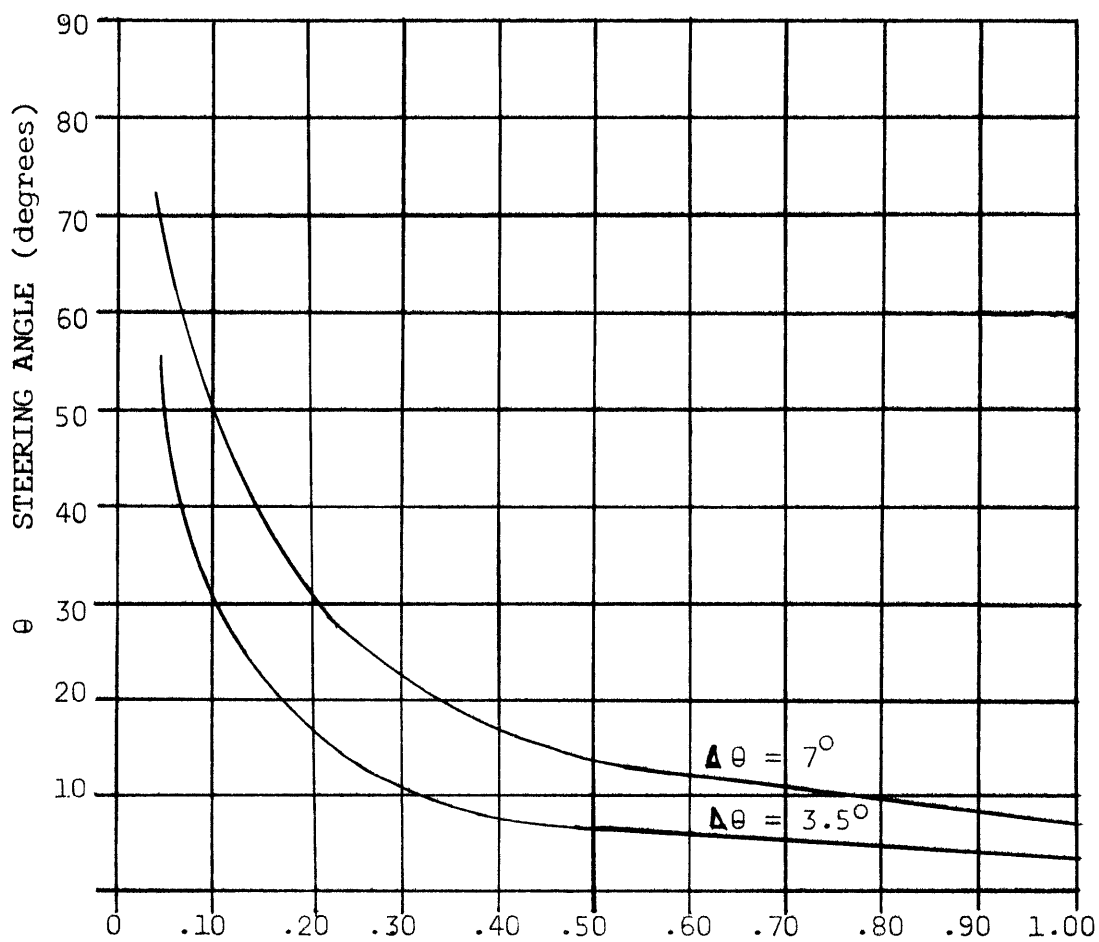
$$K(\omega) = (\frac{V(\omega)}{c_1} - 1)$$

Assume that the peak value of the sound signal strikes the first hydrophone. If the time delay was correct, this peak portion of the signal would be sampled by successive hydrophones. Each hydrophone must add the same part of the signal to give an array gain of n (for an n-element array). If the length of the array and the hydrophone spacing were such that each hydrophone added a part of the sound signal from compression through rarefaction, the hydrophone outputs would completely cancel the signal in the noise field.

The loss in array gain for the entire array equals the integral of the phase error over the array length.

$$\text{Array gain loss (in db) (normalized)} = 20 \log \left[\frac{1}{L} \int_0^L \cos \left[kx(1-c_1/V(\omega))\sin\theta \right] \right]$$

$$= 20 \log \frac{\sin \left[kL(1-c_1/V(\omega))\sin\theta \right]}{kL(1-c_1/V(\omega))\sin\theta}$$

The $20 \log \frac{\sin X}{X}$ form was plotted in Figure IX. When $X = 0$ there is no array gain loss. This happens when the phase velocity equals c_1. (The other cases for $\theta = 0$ & $L = 0$ do not apply.) Since the phase error only becomes important as a loss in array gain when $\theta = \pi/2$ (The phase error was not considered except as the error in direction $\Delta\theta$ for $\theta_1 + \Delta\theta < \frac{\pi}{2}$.), the expression simplifies to

$$\text{Loss (db)} = 20 \log \frac{\sin \left[kL(1-c_1/V(\omega)) \right]}{kL(1-c_1/V(\omega))} .$$

The loss becomes infinite when $kL(1-{}^Cl/V(\omega)) = m\pi$

$$m = (1, 2, 3, ---).$$

A useful antenna parameter was introduced previously as $D \doteq \dfrac{2kL}{\pi}$ (directivity at endfire).

Thus, Loss (db) = 20 log $\dfrac{\sin\left[\dfrac{D\pi}{2}(1-{}^Cl/V(\omega))\right]}{\dfrac{D\pi}{2}(1-{}^Cl/V(\omega))}$

The complete loss condition can now be written

$$D(1-{}^Cl/V(\omega)) - 2m \qquad m = 1, 2, ---$$

This characteristic requires the definition of a critical angle, θ_{crit}, where further electronic steering towards endfire causes array gain loss.

$$\theta_{crit} + \Delta\theta = \frac{\pi}{2}$$

$$\theta_{crit} = \frac{\pi}{2} - \Delta\theta$$

$$\theta_{crit} = \frac{\frac{\pi}{2}}{K(\omega)} - \frac{\theta_{crit}(rad)}{K(\omega)}$$

This expression may be solved graphically as the intercept of the tangent curve and a line of vertical intercept $\dfrac{\pi/2}{K(\omega)}$ and negative

42

Figure VIII

GRAPHICAL SOLUTION SHOWING THE CRITICAL STEERING
ANGLE θcrit FOR LOSS OF ARRAY GAIN: Line and Curve
Intersection Projected on the Horizontal Axis Gives θcrit
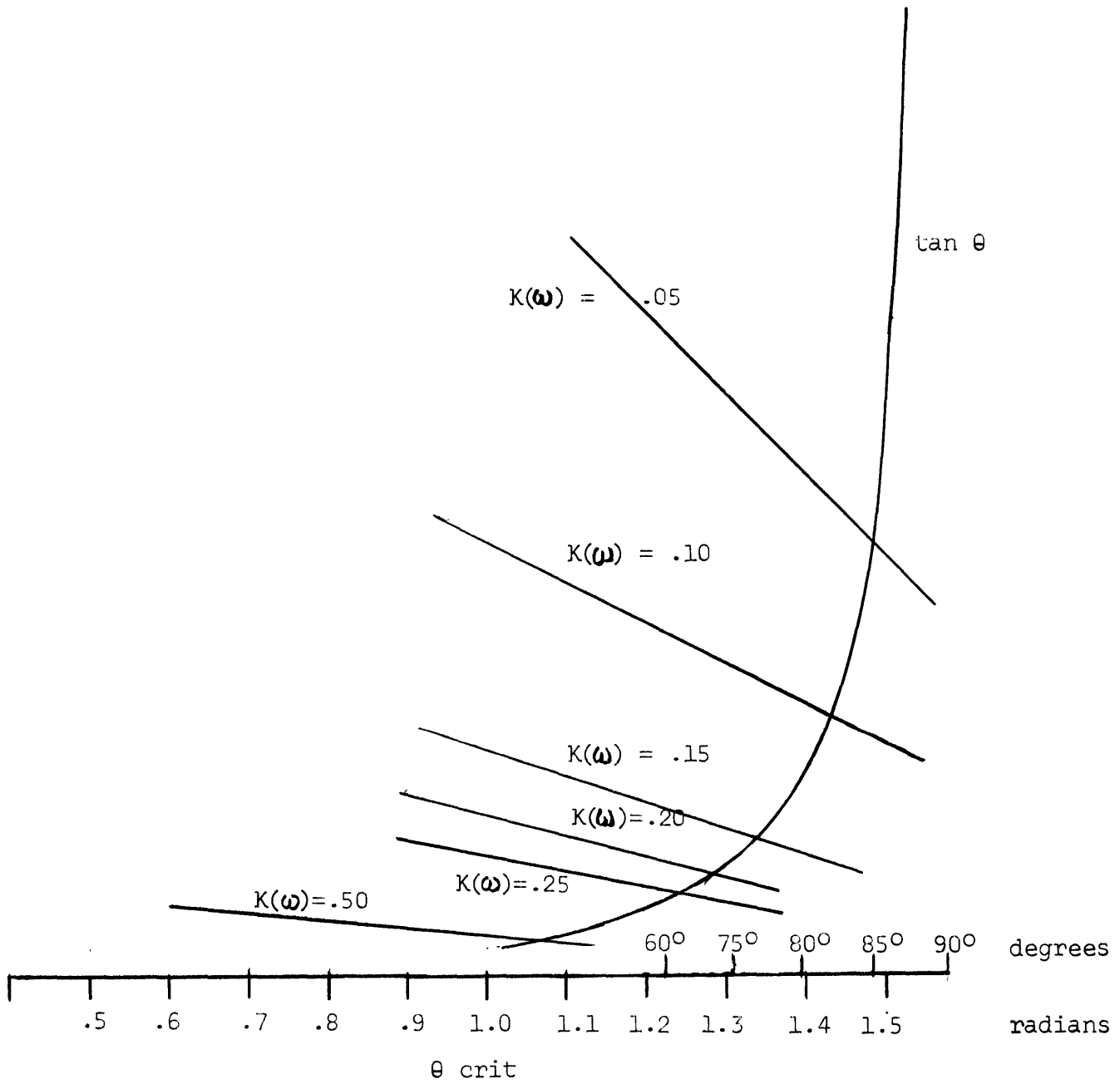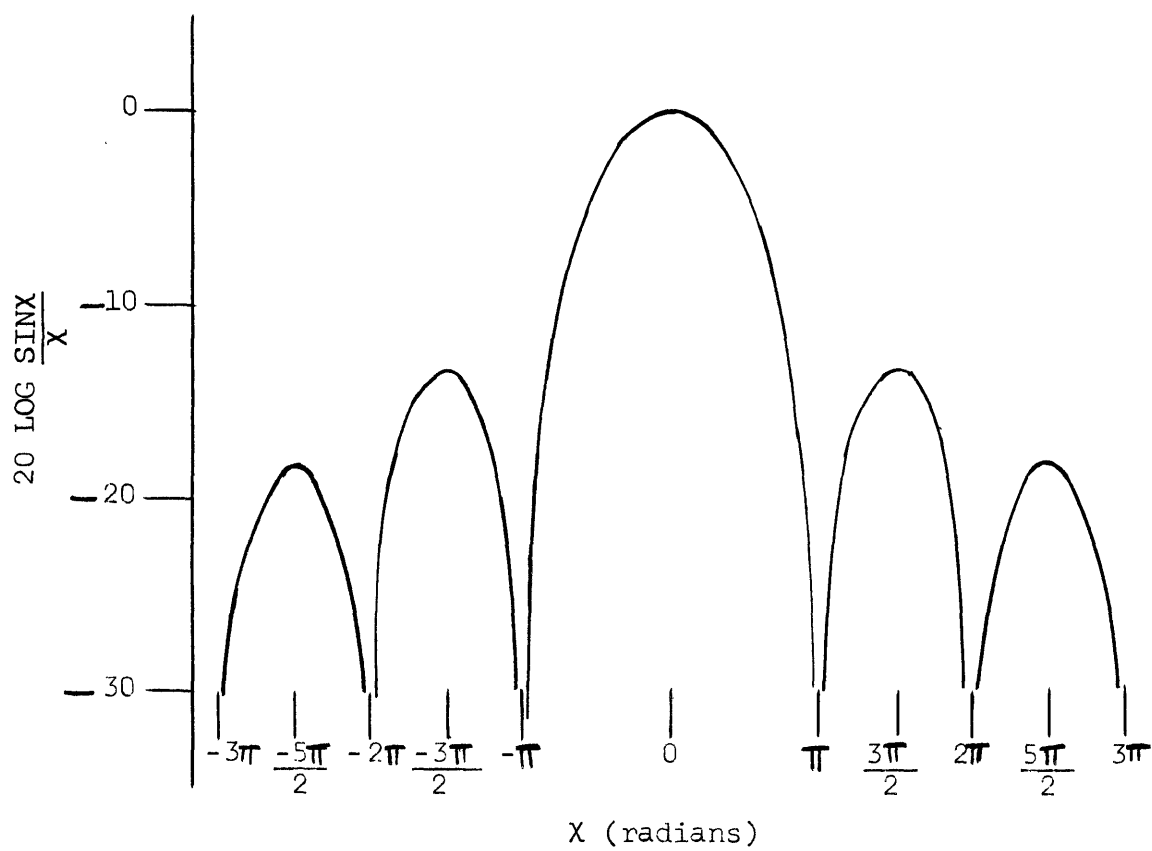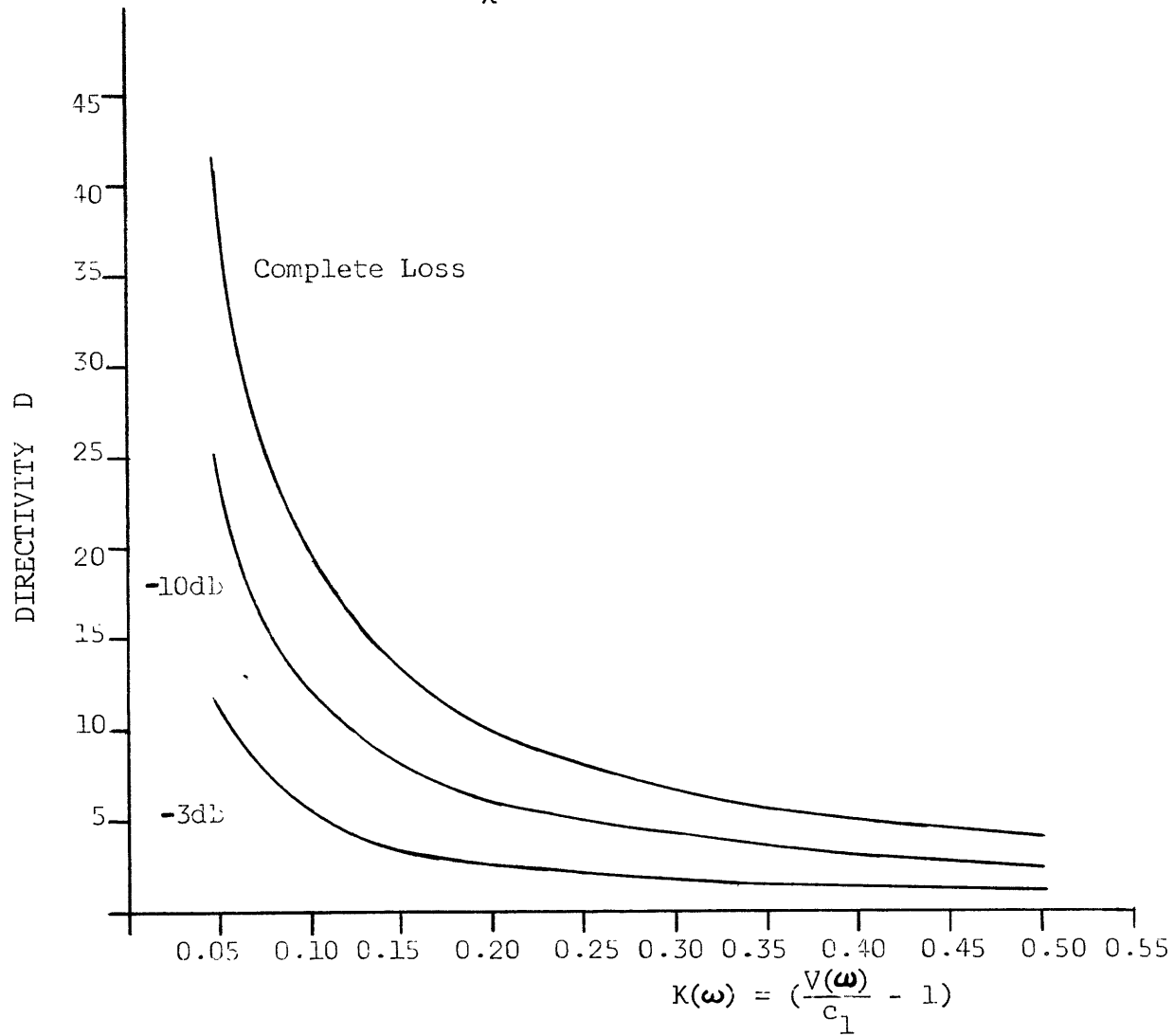
Figure IX

PLOT OF 20 LOG $\frac{SINX}{X}$ versus X

LOSS OF ARRAY GAIN FOR SOUND SOURCES AT ENDFIRE:
Function of Antenna Directivity and K(ω) for
the First 20 log $\frac{SINX}{X}$ Lobe from Figure IX

Complete Loss

-10db

-3db

DIRECTIVITY D

45
40
35
30
25
20
15
10
5

0.05 0.10 0.15 0.20 0.25 0.30 0.35 0.40 0.45 0.50 0.55

$$K(\omega) = (\frac{V(\omega)}{c_1} - 1)$$

slope $\frac{\theta}{K(\omega)}$ (radians). The point of interception projected on the
horizontal axis gives the θ_{crit} value. This graph and a graph
showing array gain loss as a function of directivity and $K(\omega)$ are
presented in Figures VIII and X. The graph in Figure X only
gives the array gain loss to the first condition of complete loss.
The peak value of array gain after this condition is approximately
-13db from the peak as seen in Figure IX.

Conclusions

The discussion has only dealt with sound sources of one discrete
frequency. The problems of an antenna system in shallow water
increase when the sound source spectrum is comprised of several
frequencies. There are essentially five characteristics predicted
by this model.

1. Since the phase velocity differs with frequency,
   "parts" of the sound signal corresponding to the
   component frequencies travel with different phase
   velocity.

2. The change in phase velocity with frequency causes
   different values of $\Delta\theta$, and this causes the sound
   signal to appear at many bearings from the array
   simultaneously.

3. Since modes travel with different velocities,
   the same frequency (if it is high enough to
   travel in more than one mode) appears at different
   bearings.

4. The sound source may seem to disappear and
   reappear at a particular angle (this angle is θ,
   just greater than θ_{crit} where loss in array
   gain begins) if the array has a sufficiently
   high directivity and the sound signal moves
   across endfire from θ_{crit} to $180-\theta_{crit}$.

5. If a frequency analysis is performed on the
   antenna output, it follows from (4) that some
   frequencies may vanish while others remain.
   This occurs since θ_{crit} varies with frequency
   and mode.

Using Figures II-V with knowledge of the operating frequency,
water depth, and ρ_1/ρ_2 and c_1/c_2 ratios, the effects of dispersion
can be found by reading the corresponding $K(\omega)$ value for the
allowed modes of propagation. The possible bearing determination
errors and the array gain loss at endfire can then be found from
Figures VII and X. Before considering the use of simply-compensated
arrays over frequency ranges that will yield $\frac{\lambda_n}{H} \doteq 0.2$, the ocean
floor velocity should be experimentally determined to allow the
estimate of possible dispersion effects.

The approximation, however, drawn in Figure VI demonstrates
that an assumed value of c_2/c_1 can give values of $K(\omega)$ when values
of λ_n/H are chosen. This approximation can be used for estimating
performance when c_2/c_1 is not definitely known; but, the designer

must remember that the cut-off frequency for unattenuated propagation cannot be found (except by later operation of the antenna system) unless this ratio is known and the depth H is known.

Finally, errors in bearing determination vanish when $\theta_1 = 0$ or when the antenna is set for broadside detection. This means that no electrical delay is used before adding the hydrophone outputs. A dispersive medium has no effect on a mechanically-steered array since the array always is looking to broadside in the electrical sense. In other words the array is no longer simply-compensated.

APPENDIX

Illustrating the Importance of the Velocity
Profile on Some Aspects of Ray Acoustics

The SOFAR channel is characterized by a sound velocity minimum.
This minimum occurs when the temperature profile is steadily
decreasing with depth and the pressure is steadily increasing. The
pressure increase raises the sound speed as the temperature decrease
lowers the sound speed. If the origin is taken at the velocity
minimum, the rays representing the propagation direction of plane
sound waves can be specified by their angle θ with the horizontal
through the origin.

Several types of curves[14] are used to represent the velocity
profile surrounding the minimum. These profiles must be examined
to see if they give the same type of sound field.

Consider a linear gradient $c(z) = c_0(1+ \beta |z|)$ where c_0 is the
minimum velocity, and z is the vertical distance from the axis.

---
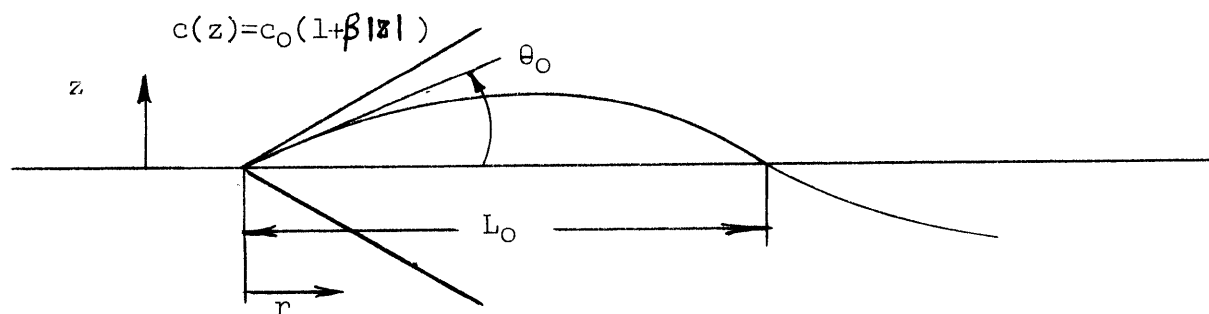
14. See Reference (2) for a more complete description.

If the source is taken at the origin, the ray is an arc of a circle of radius $\rho = \frac{1}{\beta}\sec\theta$. When $\beta > 0$ the circular arc bends upward and the curvature $K = -\beta\cos\theta_O$. The rays represent a family of circles which pass through $(r,z) = 0$ and whose centers lie on the line $z = -1/\beta$. If the velocity gradient $c_O\beta$ is positive, the ray returns to the surface $(z = 0)$ in time t_O .

$$t_O = \frac{1}{c_O\beta} \log \left[\frac{1 + \sin\theta_O}{1 - \sin\theta_O}\right] \ .$$

If the ray path follows the line $z = 0$, the travel time is

$$t_H = \frac{L_O}{c_O} \ .$$

Now the general expression for the ray path is

$(\frac{r-\tan\theta_O}{\beta})^2 + (z + 1/\beta)^2 = \frac{\sec^2\theta_O}{\beta^2}$. For the horizontal ray $(z = 0)$ the distance $L_O = \frac{2\tan\theta_O}{\beta}$. Comparing $t_O = \frac{1}{c_O\beta} \log \left[\frac{1+\sin\theta_O}{1-\sin\theta_O}\right]$ with
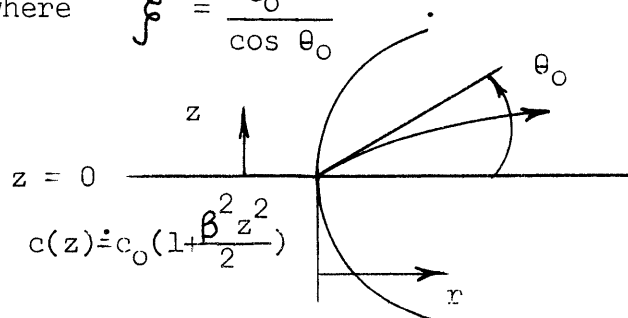
$t_H = \frac{1}{c_O\beta} 2\tan\theta_O$, it takes longer for a ray to travel the same distance over the horizontal path than by a curved ray path.

In a second case the profile is $c(z) = c_O (1- \beta^2 z^2)^{-\frac{1}{2}}$ and this is approximated as $c(z) \doteq c_O (1+ \frac{\beta^2 z^2}{2})$. In this case

$$r = \int \frac{c(z)}{\sqrt{\beta^2 - c^2(z)}} \qquad \text{where} \quad \beta = \frac{c_O}{\cos\theta_O} \ .$$

$c(z) \doteq c_O(1+\frac{\beta^2 z^2}{2})$

The equations for ray paths are $z = (^1/\beta \sin \theta_O) \sin (\beta r \sec \theta_O)$.

This is a sinusoidal wave of amplitude $1/\beta \sin \theta_O$ and a cyclic

distance ($r = A$) of $2\pi = \beta A \sec \theta_O$ where

$$A = \frac{2\pi}{\beta} \cos \theta_O \quad .$$

In general $t_A = \frac{2\pi}{c_O \beta} \left[1 - \frac{\sin^2 \theta_O}{2} \right]$ so that travel time decreases

as θ_O increases; but the distance of travel A is decreasing with

increasing θ_O. The horizontal path travel time is

$$t_H = \frac{A}{c_O} = \frac{2\pi \cos \theta_O}{c_O \beta} \quad .$$

Comparing the two cases, it is obvious since $1 - \frac{\sin^2 \theta_O}{2} > \cos \theta_O$

that the horizontal path is always faster than any curved path.

This is an opposite effect from case (1).

The third case is a combination of a minimum isovelocity area

with a linear temperature gradient.

$c = c_O(1 + (|z| + d))$

$z = 0$

c_O

d

θ_O

$z = 0$

H D_A H

r

$$\frac{H}{L} = \cos \theta_O$$
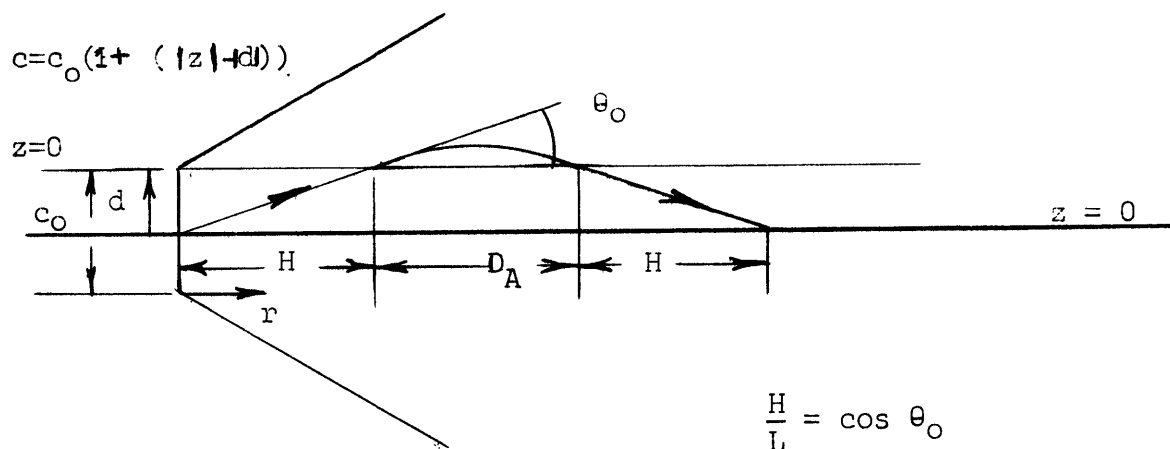
From before, the time to travel D_A is

$$t_A = \frac{1}{c_0 \beta} \log \left| \frac{1 + \sin \theta_0}{1 - \sin \theta_0} \right|$$

and the time for horizontal travel

$$t_{D_A} = \frac{2 \tan \theta_0}{c_0 \beta} \quad .$$

The time necessary to travel the inclined isovelocity paths is $t_s = \frac{2H}{c_0 \cos \theta_0}$ while the horizontal time of travel for these portions is $t_I = \frac{2H}{c_0}$. Thus

$$t_{curved} = \frac{1}{c_0 \beta} \log \left| \frac{1 + \sin \theta_0}{1 - \sin \theta_0} \right| + \frac{2H}{c_0 \cos \theta_0}$$

and

$$t_{horizontal} = \frac{2 \tan \theta_0}{c_0 \beta} + \frac{2H}{c_0} \quad \text{where } \tan \theta_0 = \frac{d}{H} \quad .$$

Now

$$\frac{2 \tan \theta_0}{c_0 \beta} > \frac{1}{c_0 \beta} \log \left| \frac{1 + \sin \theta_0}{1 - \sin \theta_0} \right|$$

and

$$\frac{2H}{c_0 \cos \theta_0} \geq \frac{2H}{c_0} \quad .$$

The travel times are equal if

$$\frac{2 \tan \theta_O}{c_O \beta} - \frac{1}{c_O \beta} \log \left[\frac{1 + \sin \theta_O}{1 - \sin \theta_O}\right] = \frac{2H}{c_O \cos \theta_O} - \frac{2H}{c_O} \quad .$$

Now

$$\frac{1}{c_O \beta} \left[2 \tan \theta_O - \log \left[\frac{1 + \sin \theta_O}{1 - \sin \theta_O}\right]\right] = \frac{2H}{c_O}\left[\frac{1}{\cos \theta_O} - 1\right]$$

and

$$\frac{1}{c_O \beta}\left[2\tan\theta_O - 2\left[\sin\theta_O + \frac{\sin^3\theta_O}{3} + - - -\right]\right] = \frac{2H}{c_O}\left[1 + \frac{\theta_O^2}{2} + \frac{5}{24}\theta_O^4 + \ldots - 1\right] \quad .$$

If $\theta_O < 1$,

$$\frac{1}{\beta}\left[2(\theta_O + \frac{\theta_O^3}{3}) - 2(\frac{\theta_O - \theta_O^3}{3!} + \frac{\theta_O^3}{3})\right] = 2H\left(\frac{\theta_O^2}{2}\right)$$

and

$$\frac{\theta_O^3}{3} = H \theta_O^2 \beta \quad .$$

Excluding the uninteresting case of $\theta_O = 0$,

$$\theta_O = \frac{H\beta}{3} \quad \text{for equal travel time by curved and horizontal}$$

paths.

Now the straight horizontal path takes longer if $\theta_o > \dfrac{H\beta}{3}$,

where $H = d \cot \theta_o$.

$$\theta_o = \frac{d(\cot \theta_o)\beta}{3}$$

$$= \frac{d\beta}{3} \left(\frac{1}{\theta_o} - \frac{\theta_o}{3} - \frac{\theta_o^3}{45} + \right) \, .$$

With θ_o taken as small

$$\theta_o = \frac{d\beta}{3} \left(\frac{1}{\theta_o} \right)$$

or $\theta_o = \sqrt{\dfrac{d\beta}{3}}$ for equal travel times.

If $\theta_o > \sqrt{\dfrac{d\beta}{3}}$, the horizontal travel time is longer. These three examples show that the relative travel times of horizontal and curved ray paths vary with the chosen SOFAR profile velocity pattern.

ACKNOWLEDGMENT

BIBLIOGRAPHY

1. Bolt, Beranek and Newman, Inc., _Directive Receiving Arrays_, Report 913, March 23, 1962, Unclassified Edition.

2. Carter, A. H., _Normal Mode Treatment of Low Frequency Acoustic Propagation in the Deep Ocean_, Bell Telephone Laboratories, Memorandum for File, January 11, 1963.

3. Carter, A. H., _Elements of Ray Acoustics_, Bell Telephone Laboratories, Memorandum for File, January 11, 1963.

4. Clay, C. S., "Array Steering in a Layered Waveguide", _Journal of the Acoustical Society of America_, 33, (865), 1961.

5. Hamilton, E. L., Shumway, Menard and Shipek, "Acoustic and Other Physical Properties of Shallow-Water Sediments off San Diego", _Journal of the Acoustical Society of America_, 28, (1), 1956.

6. Lee, Y. W., _Statistical Theory of Communication_, John Wiley and Sons, Inc., 1961.

7. Marsh, H. W. and Schulkin, _Underwater Sound Transmission_, Avco Marine Electronics Office, November, 1962.

8. Officer, C. B., _Introduction to the Theory of Sound Transmission_, McGraw-Hill Book Company, Inc., 1958.

9. _Physics of Sound in the Sea_, U. S. Department of Commerce, Office of Technical Services Report No. Pl311202.

10. Pritchard, R. L., "Approximate Calculation of the Directivity Factor of Linear Point Arrays", _Journal of the Acoustical Society of America_, 25, (1010), 1953.

11. Tolstoy, I., "Simple Harmonic Point Sources in Wave Ducts", _Journal of Acoustical Society of America_, 27, (897), 1955.